A NOVEL POWER FLOW CONTROLLER FOR CONTROLLED SERIES COMPENSATION

K.R.Padiyar, M.K.Geetha, K.U.Rao

Abstract

The Controlled Series Compensator(CSC) is a second generation FACTS device capable of providing fast, variable on line compensation. The compensation can be varied to meet various objectives such **as** control of power, damping of oscillations and improvement of stability. This paper presents a novel Constant Angle (CA) controller for power control and the results are presented with a case study.

1 INTRODUCTION

The concept of Flexible AC Transmission Systems (FACTS), was proposed by N.G.Hingorani [1] , to overcome the limitations of the present mechanically controlled AC power systems. This is acheived using fast acting and reliable thyristor controllers. The technology offers greater control of power, secure loading of lines nearer to their thermal limits and damping of power system oscillations.

The Controlled Series Compensator is a second generation FACTS device . The CSC is essentially a FC-TCR made up of one or more modules connected in series with the line, capable of providing fast variable compensation. The degree of compensation can be varied by varying the firing angle of the thyristors.

The use of fixed capacitors for increase in power transfer levels has long been in vogue. But capacitors in series with transmission lines may cause subsynchronous resonance (SSR) that can lead to electrical instability at oscillation frequencies lower than the normal system frequency resulting in spontaneous growth of oscillatory response and eventually turbine-generator shaft failure [2]. This aroused the utilities interest to determine the feasibility of the TCSC device [4].

Suitable control strategies are possible to vary the impedance of the CSC to meet various objectives such **as** power control, damping of oscillations and improvement of stability. Unlike in the case of SVC where the voltage regulation at the SVC bus is universally accepted as the basic control with supplementary control for damping, the strategy **for** the power control in the lines with CSC is yet to evolve.

This paper presents a detailed dynamic analysis of the CA controller considering various aspects including small signal Stability, transient stability and **SSR** characteristics. The performance of this novel controller is also compared with that of Constant Current (CC) controller [3]. The analysis is illustrated with the help of case studies employing IEEE second benchmark model-system 1. The results demonstrate the advantages **of** the CA controller over the CC controller.

2 SYSTEM MODELLING

Generator Model

The generator model considered here includes two circuits on the rotor (i) field winding on the direct axis and (ii) damper winding on the quadrature axis. With this model the differential equations are

$$\dot{E}'_q = \frac{1}{T'_{do}}[-E'_q + (X_d - X'_d)i_d + E_{FD}] \quad (1)$$

$$\dot{E}'_d = \frac{1}{T'_{qo}}[-E'_d - (X_q - X'_q)i_q] \quad (2)$$

The stator is represented by the two axis (d and **q** axes) equivalent of the **3** phase windings. The **flux** linkages associated with the d and q axes windings are given by

$$\frac{-1}{\omega_B}\dot{\psi}_d - (1+s_g)\psi_q - R_a i_d = V_d \quad (3)$$

$$\frac{-1}{\omega_B}\dot{\psi}_q + (1+s_g)\psi_d - R_a i_q = V_q \quad (4)$$

where s_g is the generator slip.
The rotor mechanical dynamics are represented by

$$M\frac{d^2\delta}{dt^2} = T_m - T_e \quad (5)$$

$$T_e = E'_d i_d + E'_q i_q + (X'_d - X'_q)i_d i_q \quad (6)$$

where T_m is the meclhanical torque and T_e is the electrical torque. For SSR studies, the mechanical system is described by the multi-resonant model. It is modelled as **a** linear mass-spring-damper system. A single time constant static exciter with PSS is considered as shown in Figure 1.

Network representation

The AC network consists of the generator transformer and transmission lines. It is represented by

the a-sequence network. The β-sequence network is similar to the a- sequence network. The state and output equations written for a and β sequence networks are transformed to the Kron's reference frame (D,Q frame). The CSC is represented as consisting of two parts, a fixed capacitor and a TCSC whose reactance is varied by varying the susceptance of the parallel inductor. For transient stability studies where the network transients are neglected, the network is represented by the algebraic equation

$$[Y][V] = [I] \qquad (7)$$

where, **[I]** is the vector of current injections, [V] is the vector of bus voltages and **[Y]** is the network bus admittance matrix.

3 CONTROL SCHEMES FOR THE CSC

The CSC is normally operated in the capacitive region. The CSC is operated in the inductive mode when protection of the capacitor is required. Vernier control of the CSC is possible within its reactance limits. Hence the control for the CSC is essentially meant to vary the reactance of the CSC to meet a particular objective. The constant current control reported in the literature **[3]** aims at regulating the magnitude of the current through the compensated line at a desired value , by suitably varying the reactance. In this paper, constant angle control is proposed which is aimed at regulating the voltage drop (or the phase angle) across the line. The objective is to regulate the power flow in the parallel paths particularly during contingency conditions. If $\boldsymbol{V}$ is the voltage across the line and $\hat{I}_L$ is the current flowing through the line, X_L the line reactance and $\hat{V}_{csc}$ the voltage across the CSC,then neglecting the line resistance, the control objective is

$$V = \mid I_L * X_L + V_{csc} \mid = K(constant)$$

Hence, $I_L = (K - V_{csc})/X_L = I_{,,,}$

V_{csc} is assumed to be positive in the inductive region and negative in the capacitive region. Therefore, if we choose a slope $S_k = -1/X_L$,in the control characteristic then the voltage across the line can be kept a constant. This type of control is expected to reduce the power angle swings. The steady state control characteristics for the CC and CA control can be **represented as shown in Figure 2.**

4 CONTROLLER

The controller for the CSC is shown in Figure **3** . The CSC current, $I_{,,,}$ and the voltage across the CSC, V_{csc} weighted by a factor of S_k representing the voltage droop are fed to the reference junction. T_t represents the transducer time constant assumed equal for both voltage and current measurements. The error signal I_e (the difference between the sensed current and the reference current I_{ref}) is integrated. This results in a change of the firing angle of the thyristor to appropriately correct the effective reactance of the CSC. The limits X_{cscmin} and X_{cscmax} represent the minimum and maximum values of the CSC reactance. The thyristor controller action is represented by the function $G_t(s) = \frac{1}{1+sT_s}$,where T_s is the delay time.

5 CASESTUDY

The IEEE Second benchmark model [6]shown in Fig. **4** is used for the performance evaluation of the control scheme. It consists of a single machine connected to an infinite bus through two long parallel ac lines, one of which is compensated. System data is given in the appendix.

Eigenvalue analysis is used to determine system stability and to study the effectiveness of CSC controllers on the torsional modes. The method is based on the linearization of the coupled electrical and mechanical equations under small perturbations. Linearized state and output equations are written for each subsystem described above, and then the coupling is established by the use of interface variables to get the total system '**A**' matrix.

For the system shown in Fig. **4,** Table **1** lists the eigenvalues when the line is 50% compensated i.e, $X_c = 50\%X_{L1}$, without CSC, with PSS. For this case, modes **1** and **2** are unstable. With the introduction of CSC with $X_{c1} = 25\%X_{L1}$, $X_{,,} = 15\%X_{L1}$ and $X_{,,,} = 25\%X_{L1}$ which results in total $X_{,} = 50\%X_{L1}$, mode **2** is stabilized and the negative damping of mode **1** is reduced **as** seen from Table **1.** Table 1 also lists the eigenvalues for CA and CC controls. For angle control, the gain K_I of controller is negative. From Fig. 5a which shows the variation of real part of torsional modes with K_I, with CA control, it is seen that damping of modes **2** and **1** increases with gain. Mode **1** is stabilized for gain values beyond -51. However, when the gain is zero, the net damping of mode **1** is negative mainly due to contribution of PSS. Increase in gain causes the damping of mode 0 to first decrease and then increases as seen from Fig. 5b. One of the network modes becomes unstable for gain values beyond **-54 as** shown in Fig. 5b. Thus, proper choice of controller gain leads to the stable operation **of** the **system.**

Fig.6a shows the variation of real part of torsional modes with K_I for current control. The gain is positive for current control. The eigenvalues for CC control with K_I=5 is given in Table **1.** The torsional modes **2** and **3** are stable in the range, but mode **1** is unstable. The damping of mode **1** reduces **as** the gain is increased. Figure 6b shows the root loci of mode 0 and the network mode with the lowest fre-

quency. Damping of mode 0 increases first upto a gain of 7, but further increase in gain reduces the damping. The damping of network mode decreases with increase in gain and becomes unstable for gain values beyond 7. Comparison of Figures 5a and 6a show that as the gain magnitude is increased, mode 1 is stabilized for angle control whereas the damping decreases for current control. While the network mode damping puts limits on the gain for both cases, higher gains are feasible for CA control which enables damping of all modes.

Time domain digital simulation is performed to evaluate the transient stability performance of the controller. For the simulation, the CSC is modelled as a variable reactance. The controller dynamic equations are solved to obtain the CSC reactance. The bus admittance matrix is then updated in every time step, and equation (7) is solved for the bus voltages. For the transient stability studies the infinite bus voltage is assumed to be 1.0 p.u. The mechanical torque is assumed to be constant and torsional dynamics is neglected. A three phase fault at the generator terminals, cleared in 3 cycles is considered.

Figure 7 shows the system response at 630 MW. It can be observed that the Constant Angle controller reduces the amplitude of the power angle swings as compared to the Constant Current controller. For this case the system is stable upto a power transfer level of 800 MW for constant reactance control, 730 MW with CC control and 870MW with CA control. If the excitation cointrol is not considered, then the corresponding maximum power transfer levels are 760 MW with constant reactance control, 700 MW with CC control and 840 MW with CA control.

The CA control is aimed at regulating the power in the parallel lines. Figure 8 shows the power flow in the compensated and the uncompensated lines for a minor disturbance(a small step change in the infinite bus voltage). It can be observed that the power through the uncompensated line is well modulated.

6 CONCLUSIONS

From the results of the case studies, the following conclusions can be drawn.

(i) The introduction of CSC improves the damping of the critical torsional mode as compared to the case without CSC, for the same value of percentage compensation.

(ii) The torsional rnode with lowest frequency (mode 1) is most affected as the value of controller gain is varied. For CA control, increase in the controller gain magnitude improves the damping of mode 1 and becomes stable for gain values beyond -51. For CC control,mode 1 is negatively damped with increase in controller gain. Thus CA control results in damping of the critical torsional mode.

(iii) The CA control improves transient stability limit whereas the application of fast CC control is detrimental to transient stability. This is not surprising as fast CC control prevents the flow of synchronising power in the line.

Acknowledgement:

The financial support received from the Department of Science and Technology, Government of India under the project titled, "Flexible AC Transmission Systems (FACTS) Controllers" is gratefully acknowledged.

REFERENCES

1. N.G.Hingorani,1991, " FACTS - Flexible AC Transmission Systems", IEE Fifth Int. Conf. on AC and DC transmission, London, 1-7.

2. M.C.Hall and D.A.Hodges, 1976, "Experience with 500kV subsynchronous resonance and resulting turbine generator shaft damage at Mohave generating station", IEEE PES, Winter meeting and Tesla, symposium, Publication No. 76CH1066-0-PWR, 22-29.

3. N.Christl et al., 1991, "Power system studies and modelling for the Kayenta 230kV substation advanced series compensation", IEE Fifth Int. Conf. on AC and DC transmission, London, 33-37.

4. J.Urbanek et al., 1993, "Thyristor Controlled Series Compensation prototype installation at the Slatt 500kV substation",IEEE Trans. on PWRD, 8, 1460-1469.

5. S.Nyati et al., 1994, "Effectiveness of thyristor controlled series capacitor in enhancing power system dynamics: An analog simulator study", IEEE Trans. on PWRD, 9, 1018-1027.

6. IEEE SSR Working Group, 1985, "Second benchmark model for computer simulation of subsynchronous resonance", IEEE Trans. on PAS, 104,1057-1066.

APPENDIX

Generator data(600 MVA,22kV):
f=60Hz
$x_d = 1.65$ p.u., $x'_d = 0.25$ p.u., $T'_{do} = 4.5$s
$x_q = 1.59$ p.u., $x'_q = 0.46$ p.u., $T'_{qo} = 0.55$s
AVR Data: $K_R = 200$, $T_R = 0.025$s
PSS data: $T_W = 10$s, $K_s = 12$, $T_1 = 0.048$s, $T_2 = 0.032$s.
Electrical Network (100 MVA):

R_T = 0.0002 p.u.,X_T = 0.02 p.u., R_b = 0.0014 p.u., X_b = 0.03 p.u., R_1 = 0.0074 p.u., X_{L1} = 0.08 p.u., X_c = 0.04 p.u., R_2 = 0.0067 p.u., X_{L2} = 0.0739 p.u. CSC data: Fixed compensation in one line **of** 25%, CSC capacitive reactance varies from 10% to 45%, quiescent operating value is 50%.

Mass	H (sec.)	D (p.u.)	K (p.u)
HP	0.249004	0.0498	16081.75
LP	1.55018	0.31	31435.136
GEN	0.87906	0.1758	1408.59
EXC	0.0069	0.0014	

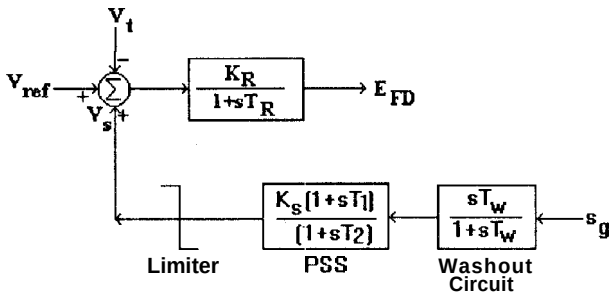

Figure **1.** Block diagram of AVR and PSS

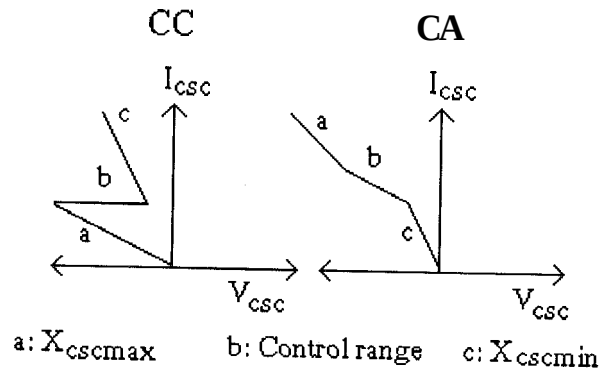

Figure 2. Steady state control characteristics

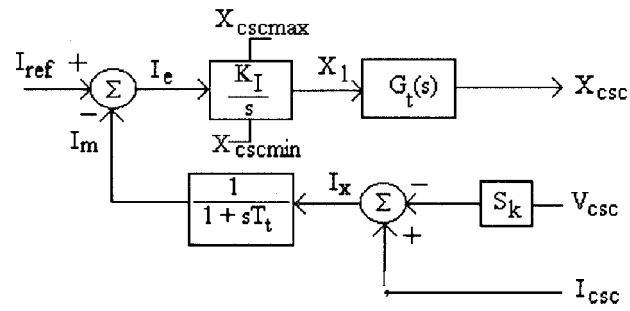

Figure **3.** CSC controller

Without CSC	With CSC			Comments
	With fixed reactance	With CA,K_I=-52	With CC,K_I=5	
-15.4704 ± j567.9755	-5.3062 ± j653.1164	-6.5515 ± j657.713	-5.2316 ± j652.897	Supersyn.
-18.926 ±j376.9356	-18.9435 **f** j376.9353	-18.9418 ± j376.938	-18.944 ± j376.935	
-0.0479 ± j321.051	-0.04786 ± j321.051	-0.0478 **f** j321.051	-0.0478 ± j321.051	Mode 3
0.0068 ± j203.3649	-0.0217 ± j203.4128	-0.0462 ± j203.429	-0.0209 ± j203.412	Mode **2**
0.3467 ± j155.4121	0.1998 ± j155.126	-0.0048 ± j155.163	0.2068 ± j155.125	Mode **1**
-2.8531 ± j10.129	-2.9777 ± j10.3231	-3.076 ± j12.643	-4.199 ± j9.526	Mode 0
-16.749 ± j19.3398	-16.692 ± j18.975	-18.38 ± j15.487	-16.021 ± j18.759	Exciter
-15.375 ± j185.859	-5.0055 ± j101.0684	-1.1662 ± j107.991	-1.116 ± j98.593	Subsyn.
-3.5511	-3.5397	-3.5456	-3.4799	
-36.1255	-36.2374	-180.7	-200.6277	
-0.1007	-0.1007	-0.1007	-0.1007	
	-10.4872 ± j507.2875	-9.5193 ± j504.653	-10.64 ± j507.6311	
	-10.4046 ± j246.6656	-0.527 ± j230.459	-11.0202 ± i247.8442	

TABLE 1. I genvalues for system in Fig. **4**

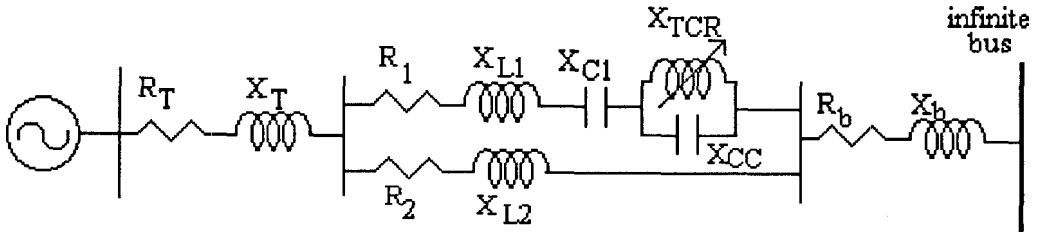

Figure 4. System under study

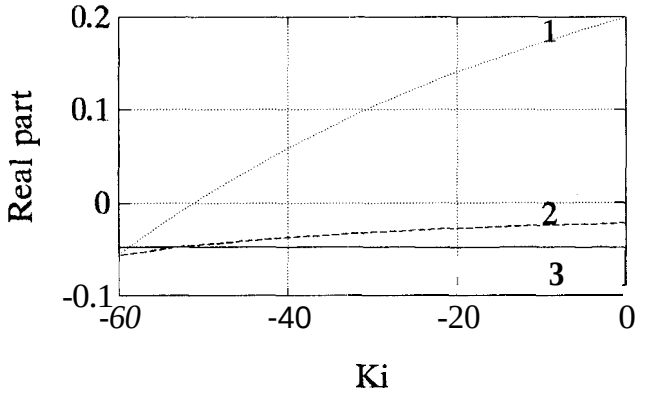

Figure 5a. Variation of real part of torsional modes with K_I, (CA)

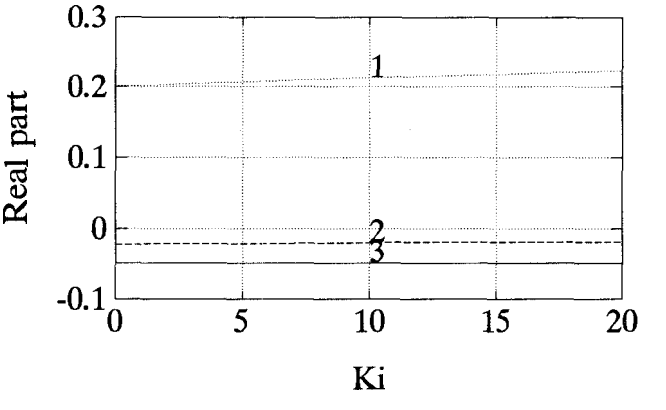

Figure 6a. Variation of real part of torsional modes with K_I, (CC)

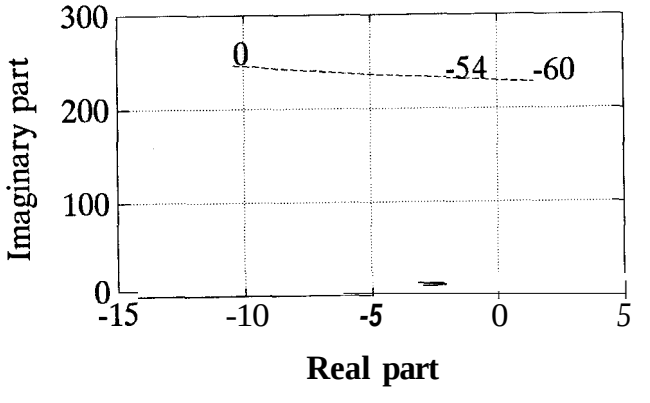

Figure 5b. Root locus of mode 0 and network mode (CA)

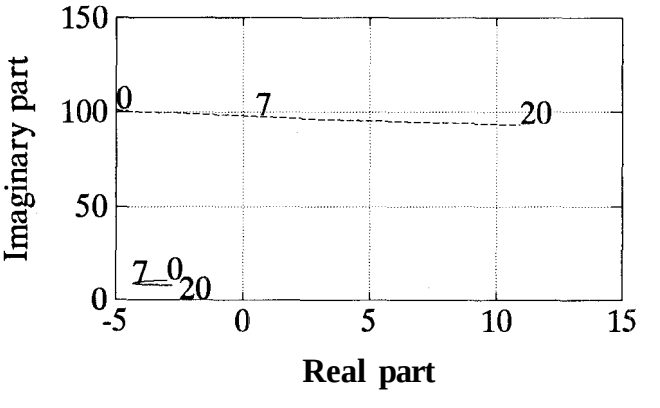

Figure 6b. Root locus of mode 0 and network mode (CC)

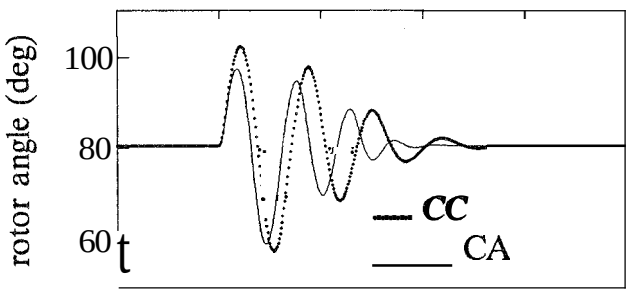

Figure 7. Swing curve

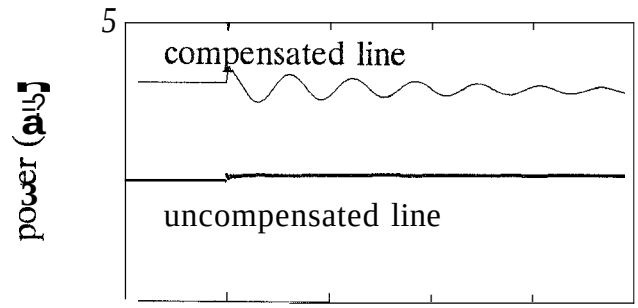

Figure 8. Power flow in the lines